Molecular Biology Reports (2023) 50:3999–4009
https://doi.org/10.1007/s11033-023-08256-0

ORIGINAL ARTICLE

Glioblastoma cell-derived exosomes induce cell death and oxidative stress in primary cultures of olfactory neurons. Role of redox stress

Yesim Yeni[1] · Ali Taghizadehghalehjoughi[2] · Sidika Genc[2] · Ahmet Hacimuftuoglu[3] · Serkan Yildirim[4] · Ismail Bolat[4]

Received: 30 October 2022 / Accepted: 4 January 2023 / Published online: 27 February 2023

Abstract

Background Glioblastoma multiforme, described as glioblastoma, is a malignancy originating from glial progenitors in the central nervous system and is the most malignant subtype of brain tumors which attracted researcher's attention due to their high recurrence and mortality despite optimal treatments. In the study, we aimed to research whether glioblastoma-originated exosomes play a role in olfactory nerve cell toxicity.

Methods and results For this aim, exosomes obtained from U373 and T98G cells were applied to olfactory nerve cell culture at distinct doses. Then, glutathione (GSH), lactate dehydrogenase (LDH), total antioxidant capacity (TAC), 3-(4,5-Dimethylthiazol-2-yl)- 2,5-diphenyltetrazolium bromide (MTT), total oxidant status (TOS) and Immunofluorescence analyzes were performed. We found that both glioblastoma-derived exosomes decreased cell viability in olfactory neurons with increasing doses. According to the obtained data, the olfactory neuron vitality rate was 71% in T98G-exosome, but the decrease in U373-exosome was more obvious (48%). In particular, the 100 µg/ml dose exacerbated oxidative stress by increasing TOS. It also increased cellular apoptosis compared to the control group due to LDH leakage. However, the results of GSH and TAS showed that antioxidant levels were significantly reduced.

Conclusion In the microenvironment of olfactory neurons, GBM-derived exosomes increased oxidative stress-induced toxicity by reducing TAC and GSH levels. Therefore, glioblastoma cells by induction of exosome-based stress support malignant growth.

Keywords Exosome · Glioblastoma · Olfactory · Neurotoxicity

Introduction

Glioblastoma multiforme (GBM), shortly described as glioblastoma, is a malignancy likely originating from glial progenitors in the central nervous system and is the most malignant subtype of a brain tumor which attracted researcher's attention due to their high recurrence and mortality despite optimal treatments [1]. The long-term survival incidence in GBM, i.e., >3 years, is between 3% to and 5% [2]. Additionally, cognitive impairment is one of the major complications of the disease in patients with gliomas [1–3]. Differing cognitive functions are significantly impaired in long-term survivors suffering from glioblastoma which is not only due to tumoral mass effect but also due to neuroinflammation [2, 4]. The decline of cognitive functioning in glioblastoma patients may also directly relate to neurotoxicity.

Indeed, in brain tumors including GBM, coculturing glioma cells and hippocampal neurons with or without direct contact causes neuronal death; yet interestingly, the excitotoxicity elicited by glioblastoma cells in these cocultures was not as high as that by glioblastoma-conditioned medium, where extracellular glutamate was allowed to accumulate freely by the release from glioblastoma cells [5]. It is not well-illuminated how these deadly malignancies induce the death of surrounding neurons. Hence, we aimed to determine

✉ Ali Taghizadehghalehjoughi
ali.tgzd@bilecik.edu.tr

1 Department of Medical Pharmacology, Faculty of Medicine, Malatya Turgut Ozal University, 44210 Malatya, Turkey

2 Faculty of Medicine, Department of Medical Pharmacology, Bilecik Seyh Edebali University, 11230 Bilecik, Turkey

3 Department of Medical Pharmacology, Faculty of Medicine, Ataturk University, 25240 Erzurum, Turkey

4 Department of Pathology, Faculty of Veterinary Medicine, Ataturk University, 25240 Erzurum, Turkey

whether exosomes are involved in glioblastoma-induced neuronal death which may contribute to versatile pathologies in these tumors including cognitive deterioration, direct facilitation of tumor growth, induction of seizures, and even peritumoral edema. Previously, microvesicles shed from G26/24 oligodendroglioma cells were found to contain pro-apoptotic proteins Fas-L and TRAIL and to induce apoptosis of neurons and benign astrocytes [6]. But, to the best of our knowledge, the effects of glioblastoma exosomes were not studied by regarding this aspect.

Exosomes are nano-sized (~30–150 nm in diameter) extracellular vesicles released by cells for cellular homeostasis and intercellular communication. Compared to exosomes, microvesicles are bigger (~0.1–1.0 μm) and released by outward cytoplasmic membrane blebbing. Most cell types, including malignant cells, release exosomes that carry distinct molecules and cargo with respect to their respective benign cells [7]. The majority of the lipids in exosomes include cholesterol, sphingomyelin, phospholipids; and triglycerides, indicating that exosomal membranes harbor lipid raft-like domains. The cholesterol level in exosomes from malignant cells contains much higher levels of cholesterol than the benign counterparts which may provide higher stability in the extracellular microenvironment [8]. As farnesylated ras can induce apoptosis in PC12 pheochromocytoma cells during serum withdrawal, it is conceivable to propose that even oncogenic and prosurvival factors of glioblastoma cells released in exosomes may trigger cytotoxic effects in recipient cells [9]. This is also relevant to neurotrophins. Neurotrophins constitute a family of growth factors initially defined in the nervous system which support the survival of both neurons and cancer cells. Glioblastoma cells could release tropomyosin kinase B (TrkB)-containing exosomes which transfer the prosurvival resistance to other glioblastoma cells [10]. It may be presumed that TrkB-containing glioblastoma exosomes may also increase the resistance of neurons against apoptotic stimuli. Nonetheless, this may not be the case, especially in the context of motor neuron survival associated with the antioxidant enzyme SOD (superoxide dismutase). In vivo deletion of TrkB from motor neurons alleviates mutant SOD1-associated toxicity with an accompanying decrease in neuroinflammation suggesting a detrimental role of TrkB in neurons in special conditions [11]. Therefore, the prosurvival factors of glioblastoma cells supporting malignant growth may detrimentally affect healthy neurons. Indeed, this is the case that we have observed in this study and there exist many observations which could support these findings as will be discussed below.

Material method

Animals and brain tissue

One-day-old Sprague Dawley rats were purchased from the Medical Experimental Application and Research Center (Turkey, Erzurum) for primary neuron culture. The body weight of the rat pups was 5 ± 1 g. Until experimental treatment, rat pups were reared in standard cages and kept in laboratory conditions (12 h light/dark cycle and 22 ± 3 °C and 55 ± 5% humidity). Brain tissue was obtained by rapidly decapitating the rat pups. A cultural order was then established.

Primary neuron culture

This study was conducted in the Department of Medical Pharmacology at the Faculty of Medicine at Atatürk University. The rats were rapidly decapitated, the removed cortices were transferred to 5 mL of Hanks' Balanced Salt solution, macro fragmentation with the help of a scalpel, and then micro lysis with 0.25% Trypsin – 0.02% Ethylene diamine tetra acetic acid (EDTA) (Sigma, USA). Subsequently, cells were then centrifuged at 1200 rpm for 5 min and cell medium ((Neurobasal medium)), 2% B_{27} (Sigma, USA), 10% FBS, 0.1% antibiotic) was added. Cells, whose medium was changed every 3 days, were incubated for 10 days.

Cell culture

U373 and T98G cell lines were obtained from the Department of Medical Pharmacology of Ataturk University (Erzurum, Turkey). They were cultured in 15% fetal bovine serum (FBS) (Sigma, USA), 1% antibiotic (streptomycin, amphotericin B, and penicillin) (Sigma, USA), and dulbecco′s modified eagle′s medium - high glucose (DMEM-HG) (Sigma, USA) to produce the simultaneously differentiated tumor population from cell lines. All cell cultures were incubated at 37 °C containing 5% CO_2.

Exosome isolation

Exosomes are isolated from T98G and U373 cells. T98G and U373 cells were seeded in a fresh medium for this aim. After 80% confluency in 150 cm^2 cell culture flasks (Corning, USA), 25 mL of complete medium was added. Subsequently, the Total Exosome Isolation Reagent (Invitrogen™ Cat. 4,478,359, MA, USA) protocol for the effective isolation of exosomes was used as previously described [12]. Briefly, the conditioned medium and reagent (2:1) were mixed and incubated at 2 to 8 °C overnight. After incubation,

the samples were centrifuged at 10,000× g for 60 min at 2 °C to 8 °C to pull down the exosomes at the bottom of the tube. The pellet was then resuspended in phosphate-buffered saline (PBS) and prepared for characterization.

Exosome characterization

Scanning electron microscope (SEM) results were obtained from Atatürk University DAYTAM center. For SEM imaging, 20 µL of exosome sample was loaded on grids, and then lyophilized by the freeze-drying procedure for 1 h. Grids were Au-coated and micrographs were taken by an SEM system (Zeiss Sigma 300, Germany) at 15 kV.

Application of exosomes

Different exosome concentrations were used to evaluate the effect of exosomes from T98G and U373 cell lines on olfactory nerve cells: 1–5–10–50–100 µg/mL. Such concentrations were selected based on similar studies reported in the literature [13, 14]. To assess the toxicity of GBM-derived exosomes, different concentrations of exosomes were added to primary olfactory neuron cells that covered 80% of the 96-well. It was then incubated for 24 h. After the incubation period, MTT, TAC, TOS, GSH, and LDH analyses and immunohistochemical staining were performed. Untreated cells were used as controls for biochemical and immunofluorescence evaluations.

3-(4,5-Dimethylthiazol-2-yl)-2,5-Diphenyltetrazolium bromide (MTT) assay

To determine cell viability, 5,000 cells per well were plated into a 96-well plate and these cells were allowed to grow for 24 h. Subsequently, cells were treated with different concentrations of exosomes except for control cells. Cell viability was determined 24 h later with the MTT kit according to the manufacturer's instructions (Sigma, USA). The stock MTT solution prepared in sterile PBS was added to 96 well plates at a concentration of 10%. After incubation for 4 h in an environment containing 5% CO_2 at 37 °C, 100 µL of DMSO was added to dissolve the formazan crystals. Formazan absorbance was evaluated with an ELISA reader (MicroQuant, Reader, BioTek, Winooski, VT, USA) at 570 nm wavelength.

TAC (total antioxidant capacity)

TAC level was measured by using the Rel Assay Total Antioxidant Capacity (Rel Assay Diagnostics, Gaziantep, Turkey) commercial kit. This method is based on the oxidation of ABTS (2,2'-Azino-di- [3-aehylbenzthiazolinesulphonate) molecule to ABTS + molecule in the presence of hydrogen peroxide. ABTS radical loses its blue and green color depending on the presence of antioxidants. The antioxidants present in the sample accelerate the lightning in proportion to their concentration. The color change was evaluated by measuring at a wavelength of 660 nm. Results were expressed per µmol Trolox Equiv/mg protein.

TOS (total oxidant status)

TOS level was measured by using the Rel Assay Total Oxidant Status (Rel Assay Diagnostics, Gaziantep, Turkey) commercial kit. This method is based on the oxidants present in the sample oxidizing the Fe^{+2}-o-dianisidine complex to the Fe^{+3} ion. Fe^{+3} ion makes a colored complex with xylenol orange in an acidic environment and the color change is proportional to the concentration of oxidant molecules in the sample and can be measured spectrophotometrically. The color change was evaluated by measuring at 530 nm wavelength. The measurement was calibrated with hydrogen peroxide and results are expressed per µmol H_2O_2 Equiv/mg protein.

Lactate dehydrogenase (LDH)

LDH test is a spectrophotometric test performed to determine the damage to the cell membrane. LDH cytotoxicity test was performed by the protocol of the purchased kit (Elabscience, USA). 100 µl/well of the standard solutions and the supernatant belonging to each group were added to the 96-well plate and left to incubate for 90 min at 37 ° C in a 5% CO_2 incubator. At the end of the incubation period, the medium was removed and the agents contained in the kit were added to the wells as stated, and the procedures were performed. The LDH activity was determined by measuring the optical density value colorimetrically in the spectrophotometer at 450 nm.

Glutathione (GSH)

The method is based on the spectrophotometric measurement of sulfhydryl groups. 5,5'-dithiobis-2-nitrobenzoic acid (DTNB) is reduced with sulfhydryl groups (-SH) to give one mole of (-SH) group to one mole of 2-nitro-5 mercaptobenzoic acid. GSH determination was carried out by the protocol of the purchased kit (Elabscience, USA). The density of the yellow coloring formed was read in a spectrophotometer at a wavelength of 450 nm.

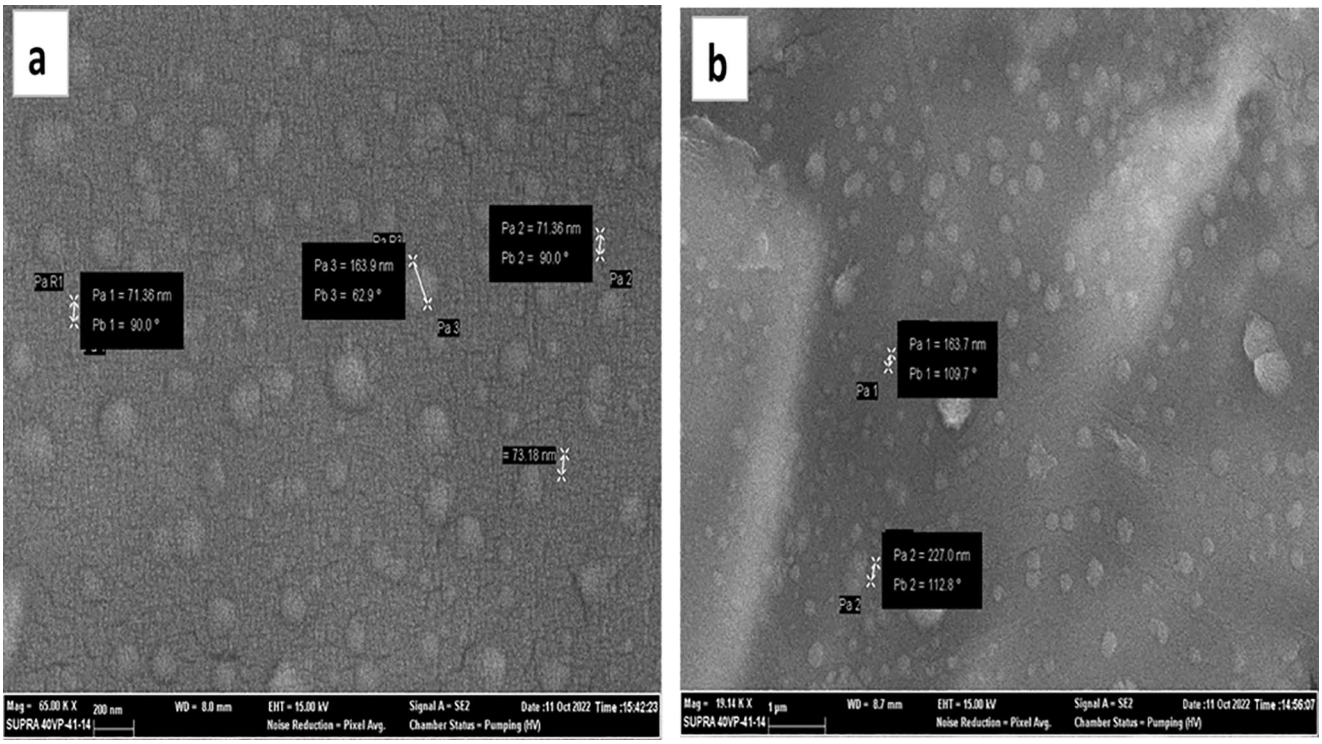

Figure 1. SEM image (a) U373 and (b) T98G-originated exosomes.

Immunohistochemical staining

For immunoperoxidase analysis, all samples in adhesive (poly-L-Lysin) plates were passed through xylol and alcohol series, deparaffinized, and dehydrated. Then they were washed in distilled water for 5 min. After fixing in paraformaldehyde for 30 min, they were washed in PBS for 5 min. Endogenous peroxidase was inactivated by keeping 3% H_2O_2 for 5 min. Primary antibodies (Cat No: ab16650 Diluent Ratio: 1/100) were prepared and dropped in appropriate dilution, kept at the appropriate temperature and time depending on the conditions of use, and washed with PBS. 8-OHdG FITC was used as the second marker (Cat No: ab6785 Diluent Ratio: 1/1000) and kept in the dark for 45 min and washed with distilled water. Subsequently, DAPI (Cat no, diluent ratio) with DNA labeling mounting medium was dropped and kept in the dark for 5 min, and the tissues were washed with distilled water and covered with a coverslip. Immunohistochemistry was followed according to the kit procedure (AbcamHRP / DAB Detection IHC kit). 3–3 'Diaminobenzidine (DAB) was used as chromogen. Ground staining was done with hematoxylin. The processed cells were examined under a fluorescence attachment microscope (Zeıss Leica DM 1000). Sections were evaluated as absent (-), very mild (+), mild (++), moderate (+++), severe (++++), and very severe (+++++) according to immune positivity.

Statistically analysis

The statistical analysis was done by using a one-way analysis of variance (ANOVA) with Tukey's HSD for post hoc comparisons using the SPSS 22.0 software. $P < 0.05$ was considered to be the statistical threshold for each analysis.

Results

Exosome characterization

SEM image showed the size of the exosomes. By using SEM imaging, a well-accepted technique for nanoparticle validation, we observed that the diameters of our particles were in the expected range for exosomes (30–150 nm). In addition, in the direction of the data obtained from the image, it was determined that the exosomes were spherical and circular structures. (Fig. 1).

Treatment with glioblastoma-originated Exosomes decrease cell viability of olfactory neurons in Vitro

The cure with U373 and T98G-originated exosomes caused a dose-dependent and statistically important exhaustion of MTT activity in olfactory nerve cells. In particular, U373-derived exosomes caused more apparent exhaustion

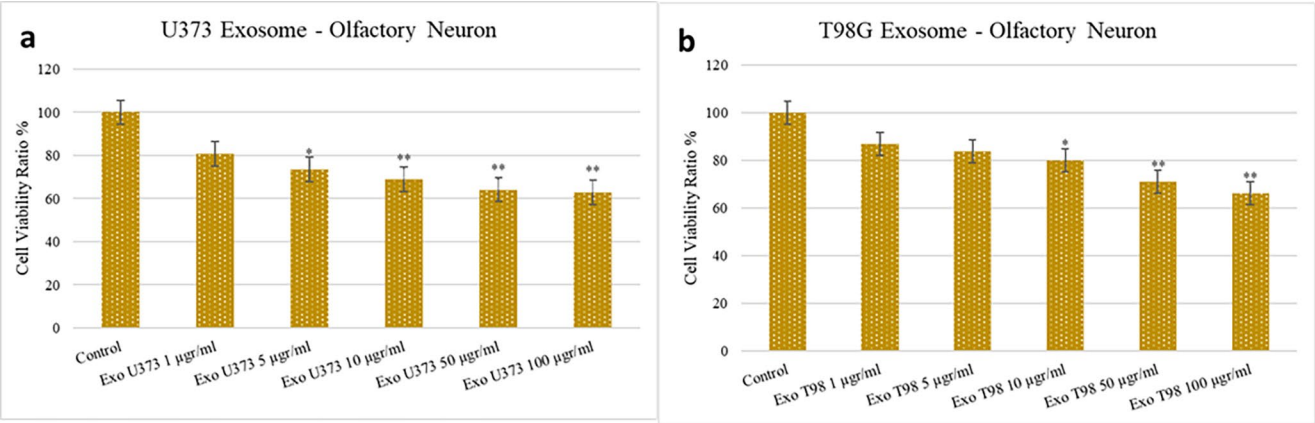

Figure 2. Reduction of olfactory neuron viability (MTT) after treatment with (a) U373- and (b) T98G-originated exosomes. ANOVA One-Way * $p < 0.05$; ** $p < 0.01$.

of MTT activity. The number of exosomes resulting from 5 µg/mL U373 exhaustion MTT was a statistically significant difference ($p < 0.05$). According to our results, cell viability decreased by approximately 53% in the 50 µg/mL U373 group and 48% in the 100 µg/mL U373. In addition, doses of 50 and 100 µg/mL more significantly depleted MTT ($p < 0.01$). Olfactory nerve cells exposed to T98G-originated exosomes showed an important decrease in cell viability ($p < 0.05$) at 10 µg/mL (79%), while a more coherent decrease in viability was observed at 50 and 100 µg/mL doses ($p < 0.01$) (Fig. 2). The most effective result was obtained at a dose of 100 µg/mL of T98G and a 71% decrease in cell viability was detected. These results show that GBM-derived exosomes have the potential to damage neuronal cells.

TAC and TOS in olfactory neurons treated with U373 and T98G-Originated exosomes

U373 and T98G-originated exosomes induced dose-dependent and a statistically important decrease in TAC. The rate of TAC exhaustion occurred with higher importance when olfactory nerve cells were exposed to T98G-originated exosomes. TAC depletion occurred at doses > 5 µg/mL of T98G-originated exosomes, with statistical importance at $p < 0.05$ and $p < 0.01$, respectively. In olfactory nerve cells exposed to U373-originated exosomes, the statistical importance of TAC exhaustion was $p < 0.05$ and $p < 0.01$ for doses of 50 and 100 µg/mL, respectively. We found the lowest TAC level in both 100 ug/ml T98 and 100 µg/mL U373 groups. With the decrease in cell viability, the antioxidant activities of neurons decreased as well (Fig. 3).

In contrast to TAC levels, the assay of TOS revealed that olfactory nerve cells treated with U373 and T98G-originated exosomes showed a statistical rise in TOS levels with a dose-dependent tendency. The rate of TOS rise was more pronounced in olfactory nerve cells exposed to U373-originated exosomes, where a statistical increase of > 5 µg/mL ($p < 0.01$ for entire doses) was observed. In olfactory nerve cells exposed to T98G-originated exosomes, TOS levels increase statistically at the 10 µg/mL dose ($p < 0.05$). At doses of 50 and 100 µg/mL, it resulted in more significant TOS levels ($p < 0.01$ for all dosages) (Fig. 3).

LDH levels in olfactory neurons after glioblastoma-originated Exosomes Treatment

U373 and T98G-originated exosomes induced a dose-dependent and statistically important rising of LDH release in the culture medium of olfactory nerve cells. Statistical significance was reached at > 5 µg/mL ($p < 0.01$ for entire doses) in olfactory nerve cells exposed to exosomes originating from both cell lines (Fig. 4). In addition, U373 exosomes increased the LDH level more significantly compared to T98G-derived exosomes. The raised levels of LDH demonstrated that the detrimental potential of glioblastoma-originated exosomes is able to induce harm in olfactory nerve cells and, as a result, nerve cell death.

Replacing of GSH levels in olfactory neurons after glioblastoma-originated Exosomes Treatment

The assay of GSH revealed a dose-dependent decrease of GSH levels in olfactory nerve cells after exposure to U373 and T98G-originated exosomes. Particularly, statistical differences in GSH levels were observed in olfactory nerve cells treated with 50 and 100 µg/mL T98G doses ($p < 0.05$) (Fig. 5). As noted, GSH exhaustion was more evident in cells exposed to U373-originated exosomes compared to T98G-originated exosomes showing a nearly 50% decrease in GSH compared to untreated cells. When compared with MTT and LDH findings, a decrease in GSH level occurred

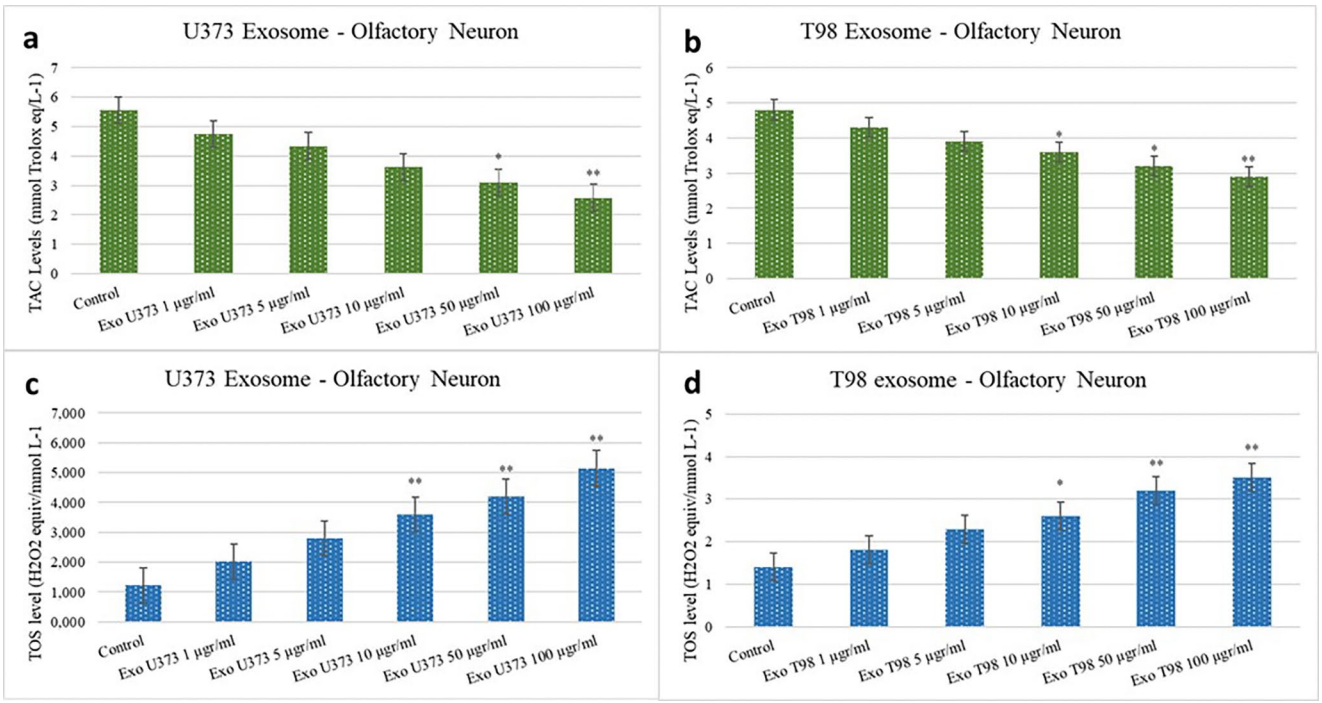

Figure 3. Reduction of TAC (a) U373- and (b) T98G- originated exosomes. and increment of TOS of olfactory neurons treated with (c) U373- and (d) T98G-originated exosomes. ANOVA One-Way *$p < 0.05$; **$p < 0.01$.

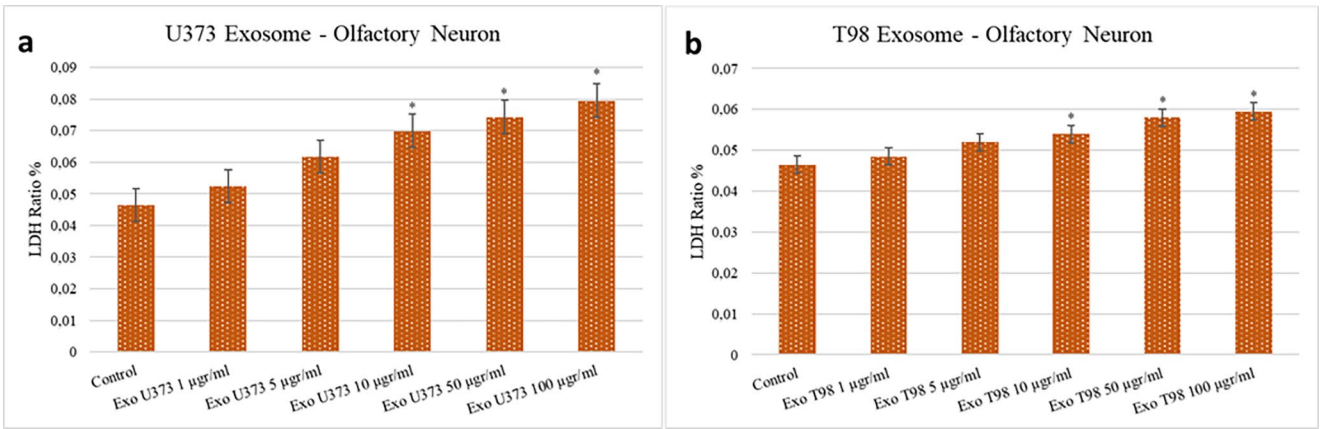

Figure 4. Significant increment of LDH levels in olfactory neurons treated with (a) U373- and (b) T98G-originated exosomes. ANOVA One-Way *$p < 0.05$; **$p < 0.01$.

in parallel with the decrease in cellular viability. Due to the increase in cellular oxidative damage, olfactory cells were driven to death, and therefore GSH level decreased.

Evaluation of immunofluorescence in olfactory neurons after glioblastoma-originated Exosomes Treatment

Sections were evaluated as absent (-), mild (+), moderate (++) and severe (+++) according to their immune positivity. According to the inflammation score, the control group was accepted as absent (-), and 100 µg/mL groups were accepted as the most severe (+++). Compared to the control group, the derived exosomes dose-dependently increased the immune expression of 8-OHdG. In particular, olfactory nerve cells exposed to the U373 exosomes were more sensitive. The decrease in the intensity of immunoreactivity in the dose groups of exosomes derived from both cell lines was statistically significant (Fig. 6). According to the 8-OHdG results, while 28.59 and 33.58 immune activities were detected in the control groups, respectively. This value was found to be 100 0.3 and 108.84 at the highest concentration. These results show that there is a significant increase in inflammation with the application of exosomes.

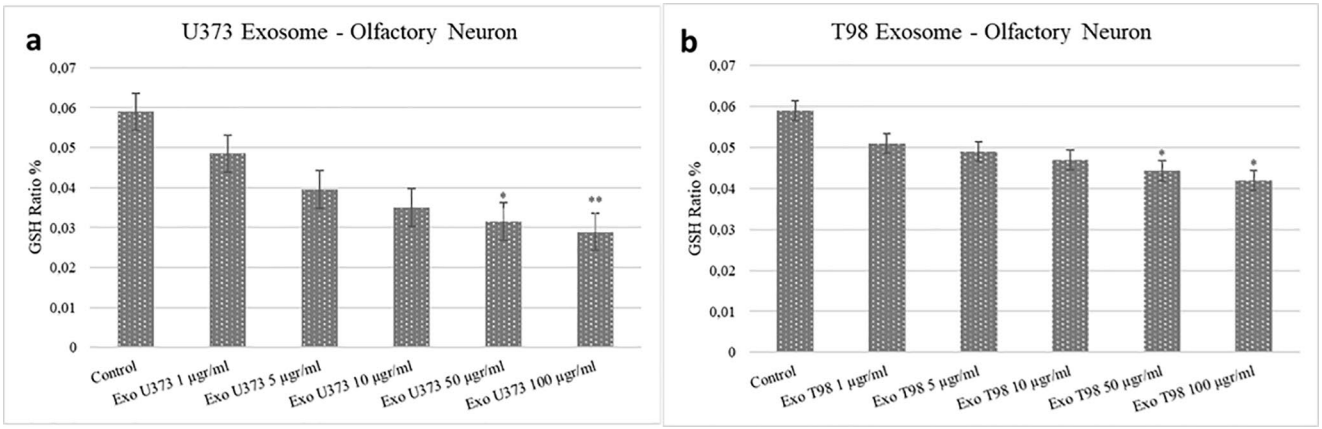

Figure 5. Significant reduction of GSH levels in olfactory neurons treated with (a) U373- and (b) T98G-originated exosomes. ANOVA One-Way *$p < 0.05$; **$p < 0.01$.

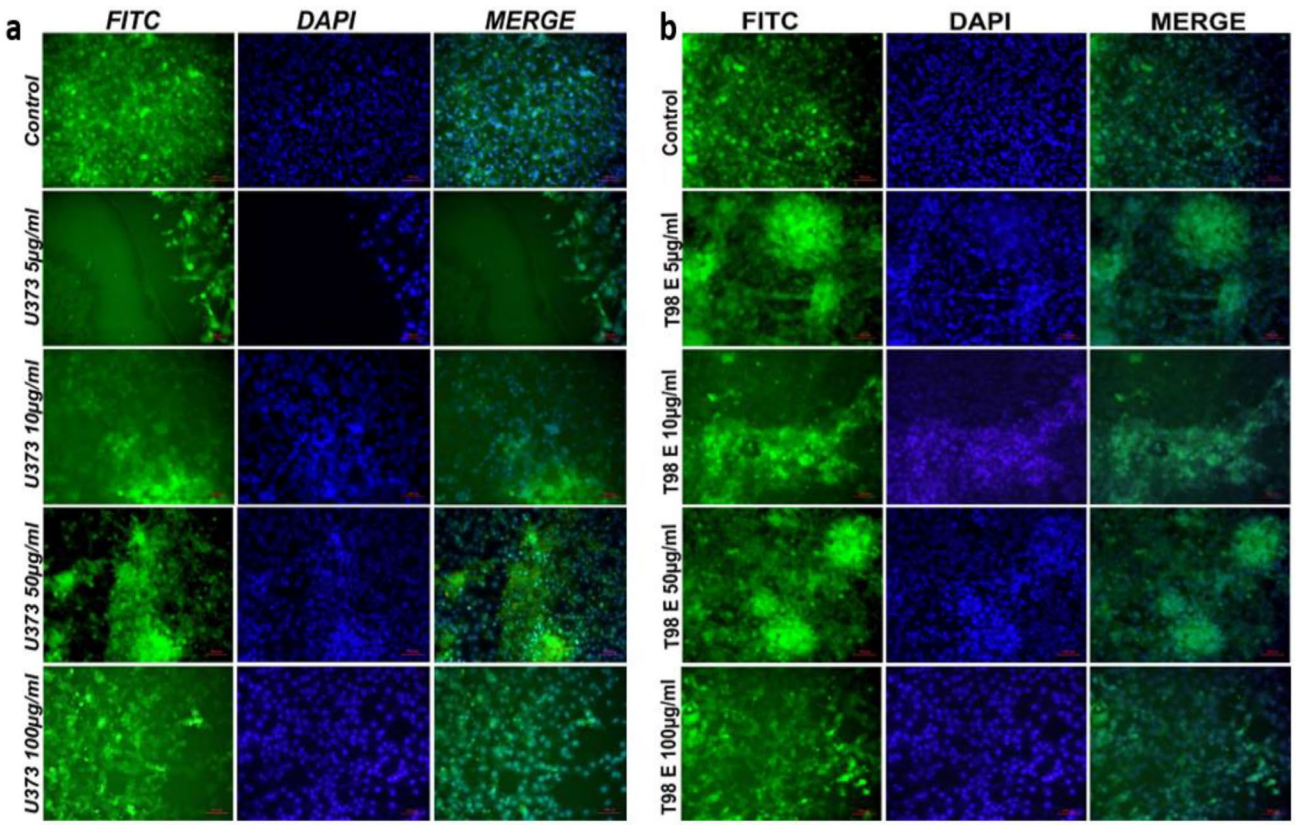

	8-OHdG	
	T98	**U373**
Control	28.59±2.49[a]	33.58±1.23[a]
5µg/ml	33.58±3[a]	37.55±2.75[a]
10µg/ml	45.12±3.38[b]	51.39±2.33[b]
50µg/ml	71.18±2.45[c]	82.6±2.06[c]
100µg/ml	100.3±2.06[d]	108.84±1.94[d]

a, b, c, d; different letters in the same column represent statistical ($p<0.05$) difference.

Figure 6. 8-OHdG and DAPI images of experimental groups. Histopathological images of Control, (a) U373 (1, 5, 10, 50, and 100 µg/ml) and (b) T98G (1, 5, 10, 50, and 100 µg/ml).

The obtained results show parallelism with cytotoxicity and oxidative stress parameters.

Discussion

Mitochondrial damage and increased production of reactive oxygen species (ROS) within malignant cells

Cancer cells exert a prooxidant shift induced by: Sustained stimulation of versatile metabolic sources of reactive oxygen species (ROS) due to the activity of NADPH oxidases (dual oxidases DUOX1/2 and NOXs), changes in energy metabolism, oxidative phosphorylation, and mitochondrial DNA (mtDNA), accompanied by glycolysis even in the presence of oxygen (Warburg effect); and lastly due to an insufficient antioxidant defense that continuously scavenges ROS produced during oncogenesis. Depending on the intracellular location and the levels, oxidant stress can induce mutations in the nuclear and mitochondrial genomes which include single or double DNA strand breaks or point mutations. There exist several factors, which contribute to the enhanced production of ROS and increased rates of DNA damage in the mitochondria of malignant cells. Mitochondrial oxidative phosphorylation is a major source of ROS, with up to 4–5% of oxygen gaining electrons directly from ubiquinol and the flavin dehydrogenases to produce superoxide anion. Mitochondrial DNA (mtDNA) is a direct target of ROS-induced injury as it is not covered by histone proteins; additionally, as mitochondria have high rates of transcription and its DNA is intronless, the chances of oxidant injury-associated mutations damaging the coding region are higher. When mtDNA is damaged, this creates further abnormalities in oxidative phosphorylation and subsequently higher mutations leading to a vicious cycle. On the other hand, a certain level of ROS is utilized as cellular signaling cascades; and malignant cells – fairly more resistant to ROS – benefit from ROS for proliferation. ROS-induced formation of glutathionylated proteins, disulfides, and cysteine sulfonic acid derivatives cause functional and conformational changes in proteins involved in cellular signaling. Only sustained and very high levels of ROS as induced by radiotherapy and chemotherapy can induce cell death and eradicate malignant cells [8]. Exosomes harbor molecular features of cells that they are released from; hence, it would be logical to propose that exosomes containing cytosolic cargo rich in ROS and oxidant stress-damaged proteins, lipids, and nucleic acids from malignant cells would trigger cell death in recipient healthy cells which uptake these exosomes.

Interplays between inflammation, glycolysis, and production of ROS. Relevance for Glioblastoma Exosomes

Numerous studies revealed the existence of inflammatory cytokines in glial tumors, peri-glioma tissues, and cerebrospinal fluid which were significantly increased than that in benign cerebral tissues, which expression levels positively correlate with the grade of glioma [1]. Hypoxia is an important factor, increasing the release of exosomes from malignant cells and there is a reciprocal stimulation of hypoxic and inflammatory pathways to produce exosomes. Interestingly, hypoxia does not reduce but rather increases the production of ROS, which in turn stimulates exosome release. Hypoxia also enhances exosomal levels of TNFα and IL-6 synthesized by tumor cells themselves [7]. However, an enhanced inflammatory feature of malignant cells is not only limited to hypoxic conditions. Glioblastoma cells inherently release high levels of TNFα which is linked to tumoral necrosis [15]. Sustained activation of inflammasome pathways such as NLRP3 also occurs in malignant cells which increases ROS production via mitochondrial damage [8]. In glioblastomas too, NLRP is involved in tumor growth and resistance to radiation therapy [16]. Moreover, cancer cells including glioblastoma act as they are in the death of oxygen even in the presence of oxygen and obtain their energy from glycolysis which is known as the Warburg effect [17]. Importantly, shikonin inhibition of glycolysis decreases the release of exosomes, while TNFα stimulates glycolysis and exosome secretion [7]. In parallel, as outlined above, the transcription factor NFκB, a downstream molecule in TNFα signaling, is involved in exosome biogenesis [18]. NFκB is induced in response to versatile stimuli in glioblastoma, which provides maintenance of cancer stem cells, enhanced invasion, mesenchymal phenotype, and radiotherapy resistance [19]. Here, it would not be illogical to propose that inflammation, hypoxia, glycolysis, and exosomes mutually increase their extent leading to a vicious cycle for the propagation of tumor growth and an increased prooxidant molecule load of exosomes.

A scenario regarding a cycle of inflammation, hypoxia, and oxidant stress is also relevant for other systemic pathological conditions and diseases. For instance, bronchoalveolar fluid-derived exosomes isolated from sarcoidosis patients induced dose-dependent increases in the release of TNF, IL-6, and IL-1β from monocytes, IFNγ from peripheral blood mononuclear cells (PBMC), IL-8 from epithelia and ROS both from monocytes and PBMC [20]. Hepatic ischemia-reperfusion injury (HIRI) following liver transplantation causes the release of chemokines, cytokines, and ROS and has detrimental effects on the life quality and prognosis of patients. It was suggested that pyroptosis and exosomes

are involved in HIRI and play important roles in neuronal death. Pyroptosis is an inflammatory programmed cell death, which is related to caspase-1 activation and the cleavage of the pore-forming protein gasdermin-D (GSDMD), formation of cell membrane cytotoxic pores, and the release of cytokines IL-18 and IL-1β. Inflammasomes are responsible for the triggering of pyroptosis. Exosomes obtained from the serum of HIRI-challenged rats cross the blood-brain barrier (BBB) and induce pyroptosis with concomitant induction of NLRP3 component of the inflammasome and production of ROS and malondialdehyde, a major lipid peroxidation production of oxidative stress [21].

Micro-RNA content of Exosomes Associated with inflammation and depletion of the antioxidant enzyme Superoxide Dismutase

Exosomes isolated from patients suffering from sepsis exerted changes in 65 miRNAs, among which 35 clustered according to survival and associated with inflammation and cell cycle regulation including pathways associated with NFκB, IL-6, Toll-Like Receptors, Glucocorticoid Receptors, and cyclins. Moreover, these exosomes also contained increased levels of mRNAs associated with oxidative stress (myeloperoxidase increased by 66 fold) and antioxidant response (Forkhead Box M1 increased by 21 fold), respectively [22]. These findings suggest that exosomes can convey both miRNAs and mRNAs which could increase inflammatory and oxidative signaling within recipient cells. It was also shown that glioblastoma cells release exosomes that contain selectively packed non-coding and coding RNAs which change gene expression in recipient cells and a high percentage of these RNAs are related to cell death and apoptosis [23]. Interestingly, high levels of exosomes released from human pancreatic cells may increase ROS production in other pancreatic cancer cells, which is increased when the exosome-donor pancreatic cancer cells are irradiated. Importantly, exosomes derived from irradiated pancreatic cancer cells contain microRNA miR-6823-5p which blocked the synthesis of SOD1 – a very potent antioxidant enzyme – and subsequently increased oxidative stress and DNA damage in recipient cells [24]. In our experimental setting, glioblastoma cells are not irradiated, but it may be still possible that the inherently high ROS load of these cells may induce the release of exosomes which would deplete SOD levels and trigger oxidative stress and death in primary neurons.

Tetraspanin proteins of Exosomes and their Association with apoptosis and ROS

CD9, CD37, CD63, CD81, CD82, and CD151 are tetraspanin proteins that are involved in biogenesis and act as markers of exosomes [7, 25]. CD9 is an analog of CD82 and both of these antigens may suppress metastasis and induce apoptosis, and CD82 is inducible with the proapoptotic and tumor suppressor gene p53 [25, 26]. While CD9 expression is increased in high-grade glial tumors and CD9 can confer maintenance of glioblastoma cells [27]; the same antigen induces apoptosis in fibrosarcoma cells and potentiates bortezomib-induced apoptosis in myeloma cells [28, 29]. Therefore, dependent on the cellular context and conditions, glioblastoma exosomal proteins may induce both cell survival and apoptosis. Peculiarly, even in the same cellular context, exosomal tetraspanins can induce simultaneous survival and death signals, such as CD37 induction of SHP-1-dependent apoptotic and PI3-Kinase-mediated prosurvival signals [30]. In the pathogenesis of diabetic nephropathy, CD63 acts as a proapoptotic factor [31]. CD81 is a proapoptotic tumor-suppressive protein in gastric cancer [32]. CD81 also stimulates apoptosis via ROS-dependent mitochondrial damage in Epstein Barr Virus-transformed B lymphocytes [33]. Hence, at least some of the tetraspanins accumulated within exosomes may partially be responsible for neuronal cell death as observed in our study.

Conclusion

To our information, this is the first work that demonstrates the toxic impacts of GBM-originated exosomes in olfactory nerve cells. The findings obtained here may explain that at least some of the tetraspanins deposited in exosomes are partially responsible for neuronal cell death as observed in our study. As noted, GSH exhaustion was more evident in cells exposed to U373-originated exosomes compared to T98G-originated exosomes showing a nearly 50% decrease in GSH compared to untreated cells. As noted, the findings here obtained are only exploratory purposes as the specific glioblastoma exosome factors involved in the neurotoxic impacts observed in olfactor nerve cells are yet unknown. However, our results will pave the way for new research studies aimed at assessing the certain molecular load of glioblastoma-originated exosomes. Indeed, more in vivo and in vitro functional works are needed to determine the major molecules responsible for neurotoxicity and to evaluate the potential therapeutical impacts of agents that can decrease tumor growth.

As a result, the prosurvival factors of glioblastoma cells supporting malignant growth may detrimentally affect

healthy nerve cells. As a matter of fact, the data we obtained in our study, describing the neurotoxic impact of glioblastoma exosomes, shows how exosomes can be evaluated both as targets and biomarkers.

Author contributions AT and YY performed the experiments and wrote the manuscript; SG, SY, and IB contributed significantly to the experiments and data analysis; AH contributed to the conception of the study.

Funding The authors did not receive any financial support.

Data Availability Data and materials are available from the authors upon request.

Declarations

Conflict of interest The authors declared no conflict of interest.

Ethical approval Animal procedures and protocols were carried out in accordance with the Animal Care and Use guidelines of Atatürk University Medical Experiment Application and Research Center. Approval was granted by the Ethics Committee of Ataturk University, Erzurum, Turkey (date of approval: 12 April 2021/protocol code no. 36643897-000-E.2100102642).

Consent to participate All individuals have signed consent forms before sample acquisition. Information on potential publications is included in consent forms signed by all individuals.

Consent for publication The participants were informed about publishing the results and they all agreed.

References

1. Li J, Liu M, Gao J, Jiang Y, Wu L, Cheong YK, Ren G, Yang Z (2020) AVNP2 protects against cognitive impairments induced by C6 glioma by suppressing tumor-associated inflammation in rats. Brain Behav Immun 87:645–659
2. Solanki C, Sadana D, Arimappamagan A, Rao KVLN, Rajeswaran J, Subbakrishna DK, Santosh V, Pandey P (2017) Impairments in quality of life and cognitive functions in long-term survivors of glioblastoma. J Neurosci Rural Pract 8(2):228–235
3. Acevedo-Vergara K, Perez-Florez M, Ramirez A, Torres-Bayona S, Dau A, Salva S, Maloof D, Garcia C, Luque M, Guillen-Burgos HF (2022) Cognitive deficits in adult patients with high-grade glioma: a systematic review. Clin Neurol Neurosurg 219:107296
4. Van Dyk K, Ganz PA (2019) The inflammation complication: new evidence in cancer-related cognitive impairment. Brain Behav Immun 81:6–7
5. Strong AD, Indart MC, Hill NR, Daniels RL (2018) GL261 glioma tumor cells respond to ATP with an intracellular calcium rise and glutamate release. Mol Cell Biochem 446(1–2):53–62
6. Lo Cicero A, Schiera G, Proia P, Saladino P, Savettieri G, Di Liegro CM, Di Liegro I (2011) Oligodendroglioma cells shed microvesicles that contain TRAIL as well as molecular chaperones and induce cell death in astrocytes. Int J Oncol 39(6):1353–1357
7. Kumar A, Deep G (2020) Hypoxia in tumor microenvironment regulates exosome biogenesis: molecular mechanisms and translational opportunities. Cancer Lett 479:23–30
8. Manda G, Isvoranu G, Comanescu MV, Manea A, Debelec Butuner B, Korkmaz KS (2015) The redox biology network in cancer pathophysiology and therapeutics. Redox Biol 5:347–357
9. Luhtala N, Aslanian A, Yates JR 3rd, Hunter T (2017) Secreted glioblastoma nanovesicles contain ıntracellular signaling proteins and active ras ıncorporated in a farnesylation-dependent manner. J Biol Chem 292(2):611–628
10. Pinet S, Bessette B, Vedrenne N, Lacroix A, Richard L, Jauberteau MO, Battu S, Lalloué F (2016) TrkB-containing exosomes promote the transfer of glioblastoma aggressiveness to YKL-40-inactivated glioblastoma cells. Oncotarget 7(31):50349–50364
11. Zhai J, Zhou W, Li J, Hayworth CR, Zhang L, Misawa H, Klein R, Scherer SS, Balice-Gordon RJ, Kalb RG (2011) The in vivo contribution of motor neuron TrkB receptors to mutant SOD1 motor neuron disease. Hum Mol Genet 20(21):4116–4131
12. Patel GK, Khan MA, Zubair H, Srivastava SK, Khushman M, Singh S, Singh AP (2019) Comparative analysis of exosome isolation methods using culture supernatant for optimum yield, purity, and downstream applications. Sci Rep 29(1):5335
13. Monfared H, Jahangard Y, Nikkhah M, Mirnajafi-Zadeh J, Mowla SJ (2019) Potential therapeutic Effects of Exosomes Packed with a mir-21-Sponge construct in a rat model of Glioblastoma. Front Oncol 20:9:782
14. Sharma P, Mesci P, Carromeu C, McClatchy DR, Schiapparelli L, Yates JR 3rd, Muotri AR, Cline HT (2019) Exosomes regulate neurogenesis and circuit assembly. Proc. Natl. Acad. Sci. USA. 6;116(32):16086–16094
15. Jin Q, Wu P, Zhou X, Qian H, Xu W (2021) Extracellular vesicles: Novel Roles in Neurological Disorders. Stem Cells Int 2021:17
16. Zhang S, Jiang L, Hu H, Wang H, Wang X, Jiang J, Ma Y, Yang J, Hou Y, Xie D, Zhang Q (2020) Pretreatment of exosomes derived from hUCMSCs with TNF-α ameliorates acute liver failure by inhibiting the activation of NLRP3 in macrophage. Life Sci 1:246:117401
17. Wolf A, Agnihotri S, Guha A (2018) Erratum: targeting metabolic remodeling in glioblastoma multiforme. Oncotarget 5(78):34855
18. Jafari R, Rahbarghazi R, Ahmadi M, Hassanpour M, Rezaie J (2020) Hypoxic exosomes orchestrate tumorigenesis: molecular mechanisms and therapeutic implications. J Transl Med 18(1):474
19. Ji J, Ding K, Luo T, Zhang X, Chen A, Zhang D, Li G, Thorsen F, Huang B, Li X, Wang J (2021) TRIM22 activates NF-κB signaling in glioblastoma by accelerating the degradation of IκBα. Cell Death Differ 28(1):367–381
20. Wahlund CJE, Gucluler Akpinar G, Steiner L, Ibrahim A, Bandeira E, Lepzien R, Lukic A, Smed-Sörensen A, Kullberg S, Eklund A, Grunewald J, Gabrielsson S (2020) Sarcoidosis exosomes stimulate monocytes to produce pro-inflammatory cytokines and CCL2. Sci Rep 10(1):15328
21. Zhang L, Liu H, Jia L, Lyu J, Sun Y, Yu H, Li H, Liu W, Weng Y, Yu W (2019) Exosomes mediate hippocampal and cortical neuronal ınjury ınduced by hepatic ıschemia-reperfusion ınjury through activating pyroptosis in rats. Oxid Med Cell Longev. 2019:3753485
22. Real JM, Ferreira LRP, Esteves GH, Koyama FC, Dias MVS, Bezerra-Neto JE, Cunha-Neto E, Machado FR, Salomão R, Azevedo LCP (2018) Exosomes from patients with septic shock convey miRNAs related to inflammation and cell cycle regulation: new signaling pathways in sepsis? Crit Care 22(1):68
23. Li CC, Eaton SA, Young PE, Lee M, Shuttleworth R, Humphreys DT, Grau GE, Combes V, Bebawy M, Gong J, Brammah S, Buckland ME, Suter CM (2013) Glioma microvesicles carry selectively packaged coding and non-coding RNAs which alter gene expression in recipient cells. RNA Biol 10(8):1333–1344
24. Nakaoka A, Nakahana M, Inubushi S, Akasaka H, Salah M, Fujita Y, Kubota H, Hassan M, Nishikawa R, Mukumoto N, Ishihara T, Miyawaki D, Sasayama T, Sasaki R (2021) Exosome-mediated

radiosensitizing effect on neighboring cancer cells via increase in intracellular levels of reactive oxygen species. Oncol Rep 45(4):13
25. Malla RR, Pandrangi S, Kumari S, Gavara MM, Badana AK (2018) Exosomal tetraspanins as regulators of cancer progression and metastasis and novel diagnostic markers. Asia Pac J Clin Oncol 14(6):383–391
26. Yunusova NV, Tugutova EA, Tamkovich SN, Kondakova IV (2018) [The role of exosomal tetraspanins and proteases in tumor progression]. Biomed Khim 64(2):123–133
27. Podergajs N, Motaln H, Rajčević U, Verbovšek U, Koršič M, Obad N, Espedal H, Vittori M, Herold-Mende C, Miletic H, Bjerkvig R, Turnšek TL (2016) Transmembrane protein CD9 is glioblastoma biomarker, relevant for maintenance of glioblastoma stem cells. Oncotarget 7(1):593–609
28. Chen S, Sun Y, Jin Z, Jing X (2011) Functional and biochemical studies of CD9 in fibrosarcoma cell line. Mol Cell Biochem 350(1–2):89–99
29. Hu X, Xuan H, Du H, Jiang H, Huang J (2014) Down-regulation of CD9 by methylation decreased bortezomib sensitivity in multiple myeloma. PLoS ONE 9(5):e95765
30. Lapalombella R, Yeh YY, Wang L, Ramanunni A, Rafiq S, Jha S, Staubli J, Lucas DM, Mani R, Herman SE, Johnson AJ, Lozanski A, Andritsos L, Jones J, Flynn JM, Lannutti B, Thompson P, Algate P, Stromatt S, Jarjoura D, Mo X, Wang D, Chen CS, Lozanski G, Heerema NA, Tridandapani S, Freitas MA, Muthusamy N, Byrd JC (2012) Tetraspanin CD37 directly mediates transduction of survival and apoptotic signals. Cancer Cell 21(5):694–708
31. Zhang RD, Shi M (2020) Occurrence and development of diabetic nephropathy caused by CD63 by inhibiting Wnt-β-catenin signaling pathway. Eur Rev Med Pharmacol Sci 24(1):284–294
32. Yoo TH, Ryu BK, Lee MG, Chi SG (2013) CD81 is a candidate tumor suppressor gene in human gastric cancer. Cell Oncol (Dordr) 36(2):141–153
33. Park GB, Kim D, Park SJ, Lee HK, Kim JH, Kim YS, Park SG, Choi IH, Yoon SH, Lee YJ, Paeng S, Hur DY (2015) Pre-stimulation of CD81 expression by resting B cells increases proliferation following EBV infection, but the overexpression of CD81 induces the apoptosis of EBV-transformed B cells. Int J Mol Med 36(6):1464–1478